Natural killer cells inhibit *Plasmodium falciparum* growth in red blood cells via antibody-dependent cellular cytotoxicity

Gunjan Arora,[1] Geoffrey T. Hart,[1,2] Javier Manzella-Lapeira,[1] Justin Y.A. Doritchamou,[3] David L. Narum,[3] L. Michael Thomas,[1] Joseph Brzostowski,[1] Sumati Rajagopalan,[1] Ogobara K. Doumbo,[4] Boubacar Traore,[4] Louis H. Miller,[5] Susan K. Pierce,[1] Patrick E. Duffy,[3] Peter D. Crompton,[1] Sanjay A. Desai,[5] and Eric O. Long[1]*

[1]Laboratory of Immunogenetics, National Institute of Allergy and Infectious Diseases, National Institutes of Health, Rockville, MD 20852, USA

[2]Department of Medicine, University of Minnesota, Minneapolis, Minnesota, USA

[3]Laboratory of Malaria Immunology and Vaccinology, National Institute of Allergy and Infectious Diseases, National Institutes of Health, Rockville, MD 20852, USA

[4]Malaria Research and Training Centre, Department of Epidemiology of Parasitic Diseases, International Center of Excellence in Research, University of Sciences, Techniques and Technologies of Bamako, Bamako, Mali

[5]Laboratory of Malaria and Vector Research, National Institute of Allergy and Infectious Diseases, National Institutes of Health, Rockville, MD 20852, USA

*For correspondence: eLong@nih.gov

Abstract

Antibodies acquired naturally through repeated exposure to *Plasmodium falciparum* are essential in the control of blood-stage malaria. Antibody-dependent functions may include neutralization of parasite–host interactions, complement activation, and activation of Fc receptor functions. A role of antibody-dependent cellular cytotoxicity (ADCC) by natural killer (NK) cells in protection from malaria has not been established. Here we show that IgG isolated from adults living in a malaria-endemic region activated ADCC by primary human NK cells, which lysed infected red blood cells (RBCs) and inhibited parasite growth in an in vitro assay for ADCC-dependent growth inhibition. RBC lysis by NK cells was highly selective for infected RBCs in a mixed culture with uninfected RBCs. Human antibodies to *P. falciparum* antigens PfEMP1 and RIFIN were sufficient to promote NK-dependent growth inhibition. As these results implicate acquired immunity through NK-mediated ADCC, antibody-based vaccines that target bloodstream parasites should consider this new mechanism of action.

Introduction

Plasmodium falciparum (P.f.), the causative agent of malaria, expresses proteins that are displayed at the surface of infected red blood cells (RBCs). Some of these proteins promote sequestration of *P.f.*-infected RBCs (iRBCs) through adhesion to vascular endothelial cells (Miller, Baruch, Marsh, & Doumbo, 2002). Humans living in malaria-endemic areas generate, over years of repeated infections, antibodies (Abs) to *P.f.* proteins that contribute to the gradual protection from malaria symptoms (Boyle et al., 2015; Bull & Marsh, 2002; Cohen, Mc, & Carrington, 1961; Mayor et al., 2015; Tran et al., 2013). One of the main objectives in malaria research is to define the mechanisms by which naturally acquired Abs provide protection (Cohen et al., 1961; Crompton et al., 2014). Acquired immunity to malaria is complex as it requires a balance of parasite growth inhibition and control of inflammation (Zhou et al., 2015). Neutralizing Abs that prevent *P.f.* merozoite invasion of RBCs have been described (Douglas et al., 2011). However, as merozoites released from late-stage iRBCs rapidly invade uninfected RBCs (uRBCs), high antibody titers are likely needed for inhibition. Abs bound to iRBCs promote phagocytosis by myeloid cells, and Abs bound to merozoites activate the complement pathway (Bouharoun-Tayoun, Oeuvray, Lunel, & Druilhe, 1995; Boyle et al., 2015; Rowe, Moulds, Newbold, & Miller, 1997).

Natural killer (NK) cells constitute about 10% of peripheral blood lymphocytes. They kill virus-infected cells and tumor cells through engagement of an array of germ-line encoded co-activation receptors (Bryceson, March, Ljunggren, & Long, 2006a; Cerwenka & Lanier, 2001). In addition to their innate ability to eliminate transformed and infected cells, NK cells perform Ab-dependent cellular cytotoxicity (ADCC) through the low affinity IgG receptor FcγRIIIa (also known as CD16), thereby killing IgG-coated target cells and secreting pro-inflammatory cytokines

such as IFN-γ and TNF-α. A clear role of NK cells in contributing to protection from malaria, and whether iRBCs could be eliminated through ADCC by NK cells, have not been established (Wolf, Sherratt, & Riley, 2017). Earlier studies have described direct lysis of iRBCs by NK cells in the absence of Abs or Ab-dependent inhibition of *P. falciparum* growth by NK cells (Mavoungou, Luty, & Kremsner, 2003; Orago & Facer, 1991). However, other studies have not confirmed such results (Wolf et al., 2017). Here, we present a detailed study of the activity of primary, unstimulated human NK cells mixed with RBCs, infected or not by *P.f.*, and evaluate the NK cell responses using several different quantitative assays. We found that IgG in plasma from subjects living in a malaria-endemic region in Mali bound to iRBCs and induced their rapid lysis through NK-mediated ADCC. Naturally acquired IgG specific for the major *P.f.* antigen PfEMP1 was sufficient to promote NK-dependent inhibition of *P.f.* growth in RBCs. Our results demonstrated that primary human NK cells alone are capable of controlling parasite growth *in vitro* in response to IgG from subjects exposed to malaria. This may represent an important component of Ab-dependent clinical immunity to *P.f.* blood-stage infection that could be exploited in the development of malaria vaccines.

Results

Primary human NK cells are activated by *P.f.*-infected RBCs in presence of plasma from malaria-exposed individuals

RBCs infected with *P.f.* strain 3D7 were enriched for the presence of knobs at the RBC surface (Figure S1A). Knobs are protrusions at the surface of iRBCs that appear at the trophozoite stage. iRBC cultures were enriched for the trophozoite stage by percoll-sorbitol gradient. Enrichment was confirmed by Giemsa stain (Figure S1B). A pool of plasma from malaria-exposed adults living in a high transmission region of Mali (Mali plasma) was tested for the presence of Abs to the surface of *P.f.* 3D7-iRBCs at the trophozoite stage by flow cytometry. Adults at the Mali study site are considered 'semi-immune' to malaria, as they generally control parasitemia and rarely experience malaria symptoms (Tran et al., 2013). Abs in Mali plasma stained iRBCs but not uRBCs (Figure 1A). In contrast, Abs in a pool of serum from malaria-naïve US adults (US serum) did not bind to iRBCs any more than they did to uRBCs (Figure 1A). Binding of Abs in Mali plasma to iRBCs was confirmed by immunofluorescence microscopy (Figure 1B). Lower magnification images of mixed uRBCs and iRBCs showed that staining by Mali plasma was selective for iRBCs (Figure S1C).

We tested the reactivity of primary NK cells, freshly isolated from the blood of healthy malaria-naïve US donors, to iRBCs in the absence of Abs. NK cells did not degranulate during co-incubation with iRBCs, as monitored by staining with anti-LAMP-1 CD107a Ab (Figure 1C and 1D). As binding of FcγRIIIA to IgG alone is sufficient to induce activation of resting NK cells (Bryceson, March, Barber, Ljunggren, & Long, 2005), IgG bound to RBCs has the potential to induce NK cell degranulation and cytokine production. We first tested stimulation of NK cells in

the presence of a polyclonal serum of rabbits that had been immunized with human RBCs. Degranulation by NK cells occurred during incubation with iRBCs in the presence of rabbit anti-RBC Abs (Figure 1C and 1D). Notably, potent NK cell degranulation occurred with iRBCs in the presence of Mali plasma, whereas US serum induced degranulation in a very small fraction of NK cells (Figure 1C and 1D). NK cell expression of intracellular interferon (IFN)-γ and tumor necrosis factor (TNF)-α was also stimulated equally well by rabbit anti-RBC serum and Mali plasma, whereas US serum did not induce cytokine production (Figure 1E, 1F and S1D). These results suggested that Abs from malaria-exposed individuals activate NK cells when bound to iRBCs, which results in NK cell degranulation and production of cytokines.

Selective lysis of *P.f.*-infected RBCs by primary NK cells in the presence of plasma from malaria-exposed individuals

We next investigated whether NK cells could selectively lyse Ab-coated iRBCs without causing bystander lysis of uRBCs. uRBCs and iRBCs were labeled with either efluor450 or efluor670 dyes, which bind cellular proteins containing primary amines, and NK cells were labeled with the lipophilic dye PKH67. The three cell types were incubated together at equal numbers, and examined by live microscopy. Images were acquired in a temperature-controlled chamber every 30 seconds for several hours (Movie file M1, M2). Representative images taken at 0, 2, and 4 h are shown in Figure 2A. Quantitative analysis of cell numbers, which were determined every minute, showed that all three cell types remained at a constant ratio when incubated with US serum (Figure 2B, left panel). In contrast, NK cells selectively lysed iRBCs in the presence of Mali plasma, leaving uRBCs intact (Figure 2B, right panel). A compilation of four experiments, each performed with NK cells from a different donor, showed iRBC lysis induced by Mali plasma but

not US serum (Figure 2C, left panel), and selective lysis of iRBCs in the presence of Mali plasma (Figure 2C, right panel). The relative change in the frequency of uRBCs and iRBCs over 3 hours in the presence of US serum or Mali plasma is shown in Movie files M1 and M2. We concluded that lysis of *P.f.*-iRBCs by NK cells in the presence of plasma from malaria-exposed individuals was efficient and specific, causing minimal bystander lysis of uRBCs.

NK cells inhibit *P.f.* growth in RBCs in the presence of IgG from malaria-exposed individuals

The fraction of RBCs invaded by merozoites (also known as parasitemia) in *P.f.*-infected individuals typically ranges from 0.005 to 5% (Goncalves et al., 2014). We tested the ability of NK cells to inhibit parasite growth in an RBC culture that was set at 1% parasitemia. As the ratio of NK cells to iRBCs was set at 3:1 and 1:1, NK cells were outnumbered by a 30 to 100 fold excess of uRBCs during incubation. Cultures were maintained for 48 hours before analysis (Figure S2A). Given that iRBC cultures were synchronized at the ring stage and enriched at the trophozoite-stage, a single round of RBC rupture and reinvasion of fresh RBCs by released merozoites occurred in the next ~18 hours. *P.f.* growth was determined by counting iRBCs in blood smears. In the absence of Abs, growth inhibition was 5.69%±11.53% at an E:T ratio of 3 (Figure 2D). A similar result was obtained in the presence of US serum (4.33%±12.15%; Figure 2D). In contrast, in the presence of Mali plasma, inhibition of parasite growth was 62.56%±15.41% at an E:T ratio of 3 (Figure 2D). Strong growth inhibition occured also at an E:T ratio of 1 (Figure 2D). A much reduced inhibition occurred with Mali plasma in the absence of NK cells (11.55%±1.99%), which could be due to Ab-mediated inhibition of merozoite reinvasion. We concluded that NK cells, in the presence of plasma from malaria-exposed individuals, are capable of inhibiting blood-stage *P.f.* growth even in the presence of a 100-fold excess of uRBCs. The results further suggested that

142 maturation of trophozoites and schizonts into infectious merozoites was inhibited by NK-mediated
143 ADCC toward iRBCs.

144 The standard growth inhibition assay (GIA) (Malkin et al., 2005) was modified in order to
145 remove Abs that inhibit *P.f.* growth through neutralization of merozoites. NK cells were first co-
146 incubated with trophozoite-enriched iRBCs for 6 hours, in the presence or absence of Mali plasma.
147 Cultures were then washed to remove unbound Abs and soluble factors prior to addition of a 100-
148 fold excess of fresh uRBCs. Cultures were further incubated for 16 hours to allow for a single
149 round of merozoite release and reinvasion of uRBCs (Figure S2B). We refer to this assay for
150 inhibition by NK-mediated ADCC as GIA-ADCC. Parasitemia at the end of the experiment was
151 determined by flow-cytometry (Figure S2C). Inhibition of *P.f.* growth occurred in the presence of
152 Mali plasma but not in the presence of US serum (Figure 2E). These results showed that inhibition
153 of *P.f.* growth was due to Abs bound to iRBCs prior to the release of merozoites and the addition
154 of uRBCs, confirming the role of NK cell-mediated ADCC.

155 As NK cell-mediated ADCC triggered by FcγRIIIa is dependent on binding to IgG, we tested
156 whether IgG in Mali plasma was sufficient to promote NK-dependent inhibition of *P.f.* growth.
157 IgG purified from US serum did not bind to uRBCs (Figure S2D) or to trophozoite-stage iRBCs
158 (Figure 2F), whereas IgG purified from Mali plasma bound to iRBCs (Figure 2F) but not uRBCs
159 (Figure S2D). In the GIA-ADCC, designed to exclude merozoite neutralization as the basis for
160 inhibition, purified IgG from Mali plasma inhibited *P.f.* growth (37.59%±12.15% inhibition at an
161 IgG concentration of 1.8 mg/ml) (Figure 2G). No inhibition was observed with IgG purified from
162 US serum (Figure 2G). These results demonstrated that IgG from malaria-exposed individuals
163 promotes inhibition of *P.f.* growth in RBCs in the presence of NK cells.
164

PfEMP1 is a major target of naturally acquired antibodies that induce NK-dependent lysis of iRBCs

The *P.f.* erythrocyte membrane protein 1 (PfEMP1), which mediates parasite sequestration through binding to vascular endothelial cells, is a major target of host Ab responses (Bull & Marsh, 2002; Chan et al., 2012).We used the parasite line DC-J, which lacks PfEMP1 expression (Dzikowski, Frank, & Deitsch, 2006), to test the importance of PfEMP1 in promoting Ab-dependent NK cell activation. Staining of *P.f.* DC-J-iRBCs with Mali plasma gave a positive signal that was approximately one log less than staining of 3D7-iRBCs (Figure 3A), but greater than staining of *P.f.* DC-J-iRBCs with US serum (Figure 3B). Time-lapse imaging was used to monitor lysis of DC-J-iRBCs by NK cells in the presence of Mali plasma during co-incubation with an equal number of uRBCs (Figure 3C). NK cells did not lyse DC-J-iRBCs in the presence of Mali plasma (movie file M3). Data from 4 experiments with NK cells from different donors indicated no significant decrease in iRBCs in the presence of Mali plasma compared to US serum over the course of 3 h (Figure 3D). Therefore, residual Ab-binding in the absence of PfEMP1 (Figure 3A) was not sufficient, under the conditions used, to promote NK-mediated ADCC in the presence of Mali plasma.

We wanted to test whether the lack of lysis of *P.f.* DC-J-iRBCs by NK cells could perhaps be due to an intrinsic resistance of DC-J to NK-mediated lysis. To test it we used the rabbit anti-serum raised against human RBCs, which activated degranulation by NK cells in the presence of 3D7-iRBCs (Figure 1C, 1D). We further developed a quantitative RBC lysis assay based on hemoglobin (Hb) release into the supernatant. Maximum Hb release from RBCs was defined as Hb in detergent lysates of RBCs (Figure S3A). This control also served to compensate for the loss of Hb during *P.f.* development in RBCs, as the parasite digests some of the Hb to produce hemozoin. Severe

188 damage to RBCs, as determined by Hb release, occurred at NK cell to RBC ratios of 3:1 and 10:1,
189 after a 5 h incubation with 3D7-iRBCs in the presence of rabbit anti-RBC Abs (Figure S3B and
190 S3C). At an NK cell to iRBC ratio of 5:1, 47.16% ± 8.76% of total Hb content was released (Figure
191 3E). A small amount of Hb was released in the absence of NK cells (1.36% ±0.51%) and in the
192 absence of rabbit anti-RBC Abs (4.38%±1.65%) (Figure 3E). Similar data were obtained with
193 uRBCs under the same conditions, where 47.15%±13.1% of total Hb content was released (Figure
194 3E). We concluded that uRBCs and 3D7 *P.f.*-iRBCs were equally sensitive to NK-mediated
195 ADCC.
196 This approach gave us an opportunity to test whether DC-J-iRBCs were inherently resistant to
197 NK-mediated ADCC. Lysis assays in the presence of rabbit anti-RBC Abs and NK cells were
198 performed. The extent of Hb release (52.66%±11.34%) after incubation at an NK cell to DC-J-
199 iRBC ratio of 5:1 for 5 h was comparable to that obtained with uRBCs and 3D7-iRBCs (Figure
200 3E). Hemoglobin release in the absence of rabbit anti-human RBC Abs was minimal. Therefore,
201 we concluded that the lack of lysis of DC-J-iRBCs in the presence of Mali plasma was not due to
202 resistance to NK-dependent ADCC, but rather to the low amount of Abs bound to RBCs infected
203 with this PfEMP1-deficient parasite strain. Together, these data suggested that naturally acquired
204 Abs to PfEMP1 play a critical role in NK cell-mediated destruction of iRBCs.
205
206 **The FcγRIIIa binding site of human IgG1 Fc is required for NK-dependent lysis of *P.f.*-**
207 **infected RBCs**
208 Abs with broad reactivity against certain members of the RIFIN family of *P.f.* proteins have
209 recently been cloned from memory B cells of malaria-exposed individuals in Kenya, Mali and
210 Tanzania (Pieper et al., 2017; Tan et al., 2016). Similar to PfEMP1, RIFIN is a type of variant

antigen expressed on the surface of iRBCs. Using a *P.f.* 3D7 strain enriched for expression of RIFIN (Figure 4A), we tested NK-dependent lysis of RIFIN$^+$ iRBCs in the presence of the RIFIN-specific human monoclonal Ab MGD21. Lysis occurred during incubation with NK cells at an NK cell to iRBC ratio of 5:1 for 6 hours, as measured by Hb release (Figure 4B). Negligible lysis was observed in the absence of NK cells or in the absence of MGD21. We then tested a variant of monoclonal Ab MGD21 (MGD21-LALA), into which mutations had been introduced in the Fc to reduce binding to Fc receptors (Tan et al., 2016). Staining of iRBCs indicated that MGD21 and MGD21-LALA bound similarly to RIFIN$^+$ iRBCs (Figure 4A). However, in the presence of NK cells, only MGD21, and not MGD21-LALA, induced Hb release (Figure 4B), demonstrating that an intact Fc receptor-binding site was required for NK cell stimulation. In addition, we concluded that *P.f.* antigens other than PfEMP1 have the potential to induce NK-dependent ADCC in the presence of specific Abs.

Naturally acquired human IgG specific for pregnancy-associated VAR2CSA antigen promotes NK-dependent lysis of infected RBCs

To further define antigenic epitopes with the potential to induce NK-dependent ADCC toward *P.f.*-iRBCs, we tested polyclonal, affinity-purified IgG from rabbits that had been immunized with the Duffy binding-like 3x (DBL3x) domain of the PfEMP1 variant VAR2CSA (Obiakor et al., 2013). This rabbit IgG stained VAR2CSA-iRBCs, as measured by flow cytometry (Figure 4C). The VAR2CSA-specific rabbit IgG, but not control rabbit serum IgG, induced Hb release from VAR2CSA-iRBCs after incubation with NK cells (Figure 4D). Uninfected RBCs were not lysed in the presence of VAR2CSA-specific rabbit IgG (Figure S4A). These results showed that domain

DBL3x was accessible to Abs at the surface of VAR2CSA-iRBCs, and oriented in such a way that bound Abs could engage FcγRIIIA on NK cells.

To test the potential of naturally acquired Abs to VAR2CSA PfEMP1 to promote NK-dependent inhibition of *P.f.* growth in RBCs, we used human IgG isolated from pooled plasma of multigravid women, and affinity-purified on DBL domains of VAR2CSA PfEMP1 (Doritchamou et al., 2016). This natural IgG stained VAR2CSA-iRBCs, as measured by flow cytometry, whereas human IgG Abs against another parasite antigen, AMA1, did not (Figure 4E). NK cells were incubated with trophozoite-stage enriched RBCs infected by *P.f.* VAR2CSA for 6 h in the presence of IgG Abs. A 100-fold excess of uRBCs was added and incubation resumed for 42 h. In the presence of naturally acquired human IgG specific for VAR2CSA PfEMP1, *P.f.* growth was inhibited by 49.88%±8.49%, which was similar to inhibition obtained with rabbit anti-DBL3x IgG (60%±11.29%) (Figure 4F, S4B). No inhibition was observed in the absence of NK cells (Figure S4C). These results showed that naturally acquired Abs to PfEMP1 induce NK-mediated ADCC, which inhibits parasite growth in RBCs.

Discussion

The main objective of our study was to test whether NK cells could help control blood-stage malaria by lysing iRBCs through ADCC. Considering the essential role of Abs in conferring clinical immunity to individuals living in areas of high *P.f.* transmission (Cohen et al., 1961), and the limited efficacy of malaria vaccines tested so far, any immune effector function that depends on Abs needs to be evaluated. We provide strong evidence of Ab-dependent NK cell cytotoxicity towards *P.f.*-iRBCs in the presence of Abs from malaria-exposed individuals in Mali. NK cell responses to iRBCs and their effect on *P.f.* growth in culture were tested using primary, unstimulated human NK cells. Lysis of iRBCs by NK cells, in the presence of Abs to *P.f.* antigens exposed at the surface of iRBCs, was highly selective, leaving most uRBCs intact. NK cell-mediated ADCC inhibited *P.f.* growth in RBC cultures. Human Abs specific for a single class of *P.f.* antigens expressed at the surface of RBCs, such as PfEMP1 and RIFIN, were sufficient to induce NK cell cytotoxicity and *P.f.* growth inhibition. We propose that NK-dependent ADCC may be an effective mechanism to limit parasite growth, as it combines the powerful cytotoxicity of innate NK cells with the specificity of Abs generated by adaptive immunity.

The developmental cycle of *P.f.* in iRBCs provides a window of opportunity for Ab-dependent immune effector responses. Following merozoite invasion of RBCs, *P.f.* proteins begin to appear at the RBC surface after 16-20 hours and remain exposed until infectious merozoites are released. Once released, merozoites rapidly invade fresh RBCs (Boyle et al., 2010). Therefore, it is likely that high Ab titers are needed to neutralize merozoites and block entry into RBCs. In contrast, RBCs harboring non-infectious *P.f.*, as it progresses through trophozoite and schizont stages, display *P.f.* antigens at their surface for more than 24 hours, and ADCC responses activated by

FcγRIIIa in primary human NK cells are rapid, strong and independent of coactivation signals (Bryceson et al., 2005).

Evidence of NK cell activation and RBC lysis was obtained with three different assays: 1) NK cell degranulation and cytokine production by flow cytometry, 2) loss of intact *P.f.*-iRBCs by live imaging, and 3) RBC lysis by measurement of Hb release. NK cell degranulation in a co-culture with *P.f.*-iRBCs, selectively induced by Abs from malaria-exposed individuals, was just as strong as that obtained with rabbit polyclonal antiserum raised against human RBCs. Furthermore, using Hb-release assays and rabbit anti-RBC serum, it was possible to show that iRBCs are not inherently more resistant or sensitive than uRBCs to NK-mediated lysis. Live imaging of a coculture of NK cells, uRBCs and *P.f.*-iRBCs, in the presence of plasma from malaria-exposed individuals, revealed selective lysis of iRBCs, with no 'bystander' lysis of uRBCs.

Natural cytotoxicity of NK cells towards *P.f.*-iRBCs was not detected in our assays with resting NK cells. A recent study in humanized mice reconstituted with human lymphocytes and injected with *P.f.*-infected human RBCs, reported some lysis of *P.f.*-iRBCs by NK cells (Chen et al., 2014). It is possible that under specific stimulatory conditions, including soluble factors and contact with other cells, human NK cells exhibit natural cytotoxic responses towards *P.f.*-iRBCs. However, considering that clinical immunity to malaria depends in large part on Abs, and that development of an effective vaccine is a high priority, we chose to focus on ADCC by NK cells. Signaling in NK cells by FcγRIIIa alone, independently of other co-activation signals and of integrin-dependent adhesion, is sufficient to induce strong responses, unlike other NK activation receptors, which require synergy through combinations of co-activation receptors (Bryceson et al., 2005; Bryceson, March, Ljunggren, & Long, 2006b). The Ab-mediated activation of NK cell cytotoxicity described here is adding a strong effector mechanism to the other mechanisms by which Abs may confer

293 protection against malaria, including neutralizing Abs and Abs that activate the complement
294 pathway (Boyle et al., 2015).

295 We have shown that NK cell-mediated ADCC inhibits the growth of *P.f.* in RBC cultures in
296 the presence of Abs to *P.f.* antigens expressed at the surface of iRBCs in a standard growth
297 inhibition assay (GIA) by co-incubation of iRBCs and NK cells with a large excess of uRBCs. To
298 distinguish inhibition by NK cells from other Ab-dependent functions, such as merozoite
299 neutralization and activation of complement, we developed a two-step GIA to evaluate inhibition
300 that had occurred prior to iRBC rupture and reinvasion of fresh RBCs. As inhibition of *P.f.* growth
301 occurred in the presence of purified IgG from plasma of malaria-exposed individuals, other serum
302 components were not required for NK-mediated inhibition. The modified GIA for ADCC could
303 help define *P.f.* antigens that induce Abs of sufficient titer and quality for FcR activation (e.g. IgG
304 isotype, glycosylation). The GIA-ADCC is well-suited to large screens of plasma from subjects in
305 malaria vaccine trials or in studies of naturally acquired immunity to malaria.

306 Previous work has shown that IL-2 produced by T cells following malaria infection or injection
307 of a malaria vaccine activates IFN-γ production by NK cells (Wolf et al., 2017). In addition, *P.f.*
308 infection activates IL-18 secretion by macrophages. Through IL-18 and direct contact with
309 macrophages NK cells are activated to produce IFN-γ (Baratin et al., 2005; Wolf et al., 2017). In
310 contrast, the effector functions of NK cells we describe here are independent of external signals,
311 since unstimulated primary NK cells respond directly to activation by multivalent IgG Fc binding
312 to FcγRIIIa (Bryceson et al., 2005). Experiments performed here used NK cells freshly isolated
313 from human blood, without stimulation prior to incubation with RBCs and Abs. In summary, we
314 have shown that human NK cells have the potential to control *P.f.* parasitemia through IgG-

315 dependent activation of NK cellular cytotoxicity, and thus contribute to protection from blood-
316 stage malaria.

Materials and Methods

Study approval: This study was approved by the Ethics Committee of the Faculty of Medicine, Pharmacy, and Dentistry at the University of Sciences, Techniques, and Technologies of Bamako, in Mali and by the Institutional Review Board of the National Institute of Allergy and Infectious Diseases, National Institutes of Health. Prior to inclusion in this study, written informed consent was received from participants.

Antibody sources: Plasma samples were collected from adults enrolled in a multi-year malaria study in the rural village Kambila (Crompton et al., 2008), by starting with venous blood collected in citrate-containing cell-preparation tubes (BD, Franklin Lakes, NJ). Samples were transported 45 km away to the Malaria Research and Training Centre in Bamako, where peripheral blood mononuclear cells (PBMCs) and plasma were isolated. Plasma was frozen in 1-ml aliquots at −80°C. Samples were shipped to the United States on dry ice for analysis. Control US serum was obtained from Valley Biomedical (Winchester, VA).

Enrichment of antibody: IgG was purified from plasma or serum by standard affinity chromatography. Briefly, each sample was diluted 1:5 in column equilibration-wash buffer (10 mM $NaPO_4$, 150 mM NaCl, pH 7.0). The IgG fraction was isolated on Protein G columns (GE Healthcare, Amersham-Pharmacia-HiTrap Protein G) and eluted with 100 mM glycine, pH 2.5. and immediately neutralized to pH 7.4 with 4.0 M Tris pH 8.0. IgG was concentrated and dialyzed in Pall Macrosep columns (30 kDa MW cutoff) with PBS.

NK Cell isolation: Human blood samples from deidentified healthy US donors were drawn for research purposes at the NIH Blood Bank under an NIH IRB approved protocol with informed consent. PBMCs were first isolated using Lymphocyte Separation Medium (MP Biomedicals, Solon, OH), washed with PBS twice, and resuspended in PBS, with 2% FBS

and 1 mM EDTA. NK cells were isolated from PBMCs by depletion of non-NK cells using an NK cell isolation kit (STEMCELL Technologies, Cambridge, MA). The manufacturer's protocol was modified as follows. PBMCs were resuspended at 2×10^8, per ml and 2.5 µl/ml of anti-CD3 biotin (STEMCELL Technologies) was added to the 50 µl/ml of the non-NK cocktail to increase NK cell purity. Resting NK cells were resuspended in Iscove's modified Dulbecco's medium (IMDM; Invitrogen, Carlsbad, CA) supplemented with 10% human serum (Valley Biomedical, Winchester, VA), and were used within 1 to 4 days after isolation. Only NK cell preparations that had greater than 95% CD14neg, CD3neg, CD56pos, as determined by flow cytometry, were used in experiments.

Cultivation and purification of *P. falciparum*: 3D7 and FCR3 VAR2CSA strains were cultivated at 37°C under 5% O_2, 5% CO_2, 90% N_2 at 37°C at <5% hematocrit using O^+ human erythrocytes (Interstate Blood Bank, Inc.). The *P.f.* DC-J strain was cultivated similarly in the presence of Blasticidin (2.5 µg/ml). Parasites were cultured in complete medium, which was RPMI 1640 buffered with 25 mM HEPES and supplemented with 2.5% heat-inactivated Human AB Serum, 0.5% Albumax-II, 28 mM sodium bicarbonate, 25 µg/ml gentamycin, and 50 µg/ml hypoxanthine. Parasite development was monitored by light microscopy using methanol-fixed, Giemsa-stained thin blood films. Parasites were synchronized using sorbitol (Lambros & Vanderberg, 1979). Parasite-iRBCs were enriched for knobs using Zeptogel (contains gelatin) sedimentation routinely. Infected RBCs used in ADCC assays were enriched at the trophozoite stage with percoll-sorbitol gradient and centrifugation (Aley, Sherwood, & Howard, 1984; Hill et al., 2007), washed, and resuspended in complete medium in the absence of human serum. Cultures growing in Albumax-II therefore had no antibodies or complement components.

Immunostaining and Immunofluorescence analysis: iRBCs, enriched at the trophozoite stage, were resuspended in PBS and 2% FBS, and incubated at 4°C for 30 minutes with plasma, serum, or purified antibodies at specified dilutions. Cells were washed and incubated at 4°C with appropriate and fluorescently-tagged secondary Abs for an additional 20 minutes. Cells were washed, and flow cytometry was performed on a FACS LSR-II or a FACS Calibur (BD Biosciences), and data analyzed with FlowJo (FlowJo, LLC). For immunofluorescence analysis, iRBCs, enriched at the trophozoite stage, were mixed with uRBCs at a ratio of 1:1 and incubated with US Serum or Mali Plasma for 30 minutes at 4°C. Cells were washed and incubated with fluorescently –tagged secondary Abs for an additional 20 minutes. Cells were first washed, and then fixed with 1% paraformaldehyde (PFA) at room temperature. DAPI was used to visualize the *P.f.* DNA in iRBCs. Immunofluorescence images were obtained on a LSM 780 confocal laser microscope (Carl Zeiss, Oberkochen, Germany). Images were acquired using the Zen software (Carl Zeiss).

Scanning Electron Microscopy: uRBCs and iRBCs were washed with 0.1 M phosphate buffer (pH 7.4). RBCs were centrifuged at 2500 rpm for 5 minutes and supernatants were removed. RBCs were again washed with 0.1 M phosphate buffer (pH 7.4). RBCs were resuspended in 3 ml of fixative solution (3% PFA + 0.1% glutaraldehyde). The cells were stored at 4°C until further processing for imaging. Fixed cells were allowed to settle on silicon chips for 1 hr. Subsequent post-fixation with 1% OsO_4 was performed with microwave irradiation (Pelco 3451 microwave processor, in cycles of 2 min on, 2 min off, 2 min on at 250 W under 15 in. Hg vacuum; Ted Pella, Redding, CA). Specimens were dehydrated in a graded ethanol series for 1 min under vacuum. Samples were then dried to a critical point in a Bal-Tec cpd 030 drier (Balzer, Bal-Tec AG, Balzers, Liechtenstein). Cells were then coated with 75 Å of iridium in an IBS ion beam sputter (South

385 Bay Technology, Inc., San Clemente, CA.) Samples were imaged on a Hitachi SU-8000 SEM
386 (Hitachi, Pleasantown, CA).

387 **Degranulation and intracellular cytokine assays**: Resting NK cells (2×10^5) either alone or
388 mixed with enriched iRBCs (2×10^5) were added to wells of a 96-well plate, in the presence of
389 antibodies (either US serum diluted 1:10, Mali plasma diluted 1:10, or rabbit anti-human RBC
390 antibody at 1.25 μg/ml). Anti-CD107a Ab–PE diluted 1:20 (Clone H4A3, Cat#555801, BD
391 Biosciences, Franklin Lakes, NJ) was added at the beginning of the incubation with NK cells. Cells
392 were centrifuged for 3 minutes at 100g and incubated for 4 hours at 37°C. Cells were centrifuged,
393 resuspended in PBS containing 2% FBS, and stained with conjugated anti-CD56–PC5.5 Ab (Clone
394 N901, Beckman Coulter, Brea, CA), near-IR fixable Live/Dead dye (Invitrogen), and CD235a–
395 FITC (Clone H1264, Biolegend, San Diego, CA). Samples were analyzed on a FACS-LSRII flow
396 cytometer (BD Biosciences) and data analyzed with FlowJo software (FlowJo, LLC). For
397 intracellular cytokine assays, NK cells were incubated with iRBCs as described above in the
398 presence of Brefeldin A (5 μg/ml) during the 4 hour incubation. Cells were then stained with anti-
399 CD56–PC5.5 Ab (Clone N901, Beckman Coulter, Brea, CA), near-IR fixable Live/Dead dye
400 (Invitrogen), CD235a–FITC (Clone H1264, Biolegend, San Diego, CA), followed by fixation and
401 permeabilization using the BD Cytofix/Cytoperm Kit (BD Biosciences). IFN-γ was detected using
402 anti-IFN-γ–APC Ab (Clone B27, BD Biosciences) and TNF-α was detected using anti-TNF-α–
403 PE Ab (Clone 6401.1111, BD Bioscience). Samples were resuspended in PBS and analyzed on a
404 FACS LSRII flow cytometer (BD Biosciences). Data analysis was performed with FlowJo
405 software (FlowJo, LLC).

406 **Time-lapse imaging**: NK cells, uRBCs and iRBCs were washed twice with PBS before labeling
407 with different dyes. iRBCs were stained with cell proliferation dye efluor 670 at 5 μM for 5

minutes in PBS at 37°C. Similarly, uRBCs were stained with efluor 450 dye at 2.5 μM concentration for 5 minutes in PBS at 37°C. NK cells were washed, suspended in diluent C and stained with 1 μM PKH67 membrane dye (PKH67 green fluorescent green linker kit, Sigma-Aldrich) for 5 minutes at 37°C. Cells were then washed 3 times with media containing serum (e.g., RPMI with 10% FBS). For imaging, cells were resuspended in RPMI 1640 containing 0.5% Albumax-II in the absence of Phenol Red. Cells were added in 8-well Lab-Tek I Chambered cover glass (Nunc) and allowed to settle for 15 minutes. Imaging was performed with a Zeiss LSM 780 confocal microscope while maintaining incubation condition at 37°C, 5% CO_2, in a humidified chamber. Images were acquired at 30 seconds interval for 6 hours. Time-lapse image stacks were imported into the Imaris software. A threshold algorithm eliminated background noise from each channel, and a Gaussian filter was applied to smooth the texture, and to easily segment the regions of interest (ROIs). After filtering, a surface channel was created from each color channel for each cell population, with surface threshold based on intensity. The surface generator was set to run a watershed algorithm. The seed-points diameter was set to 4.5 μm for iRBCs and uRBCs, and 6.0 μm for NK cells. In order to weed out unwanted particles that passed the intensity threshold, a surface ROI was considered to be one with voxel size greater than 110 voxels. For the tracking algorithm we used autoregressive motion with maximum step distance set to 5 μm and maximum gap size set to 2 frames.

Growth inhibition assay (GIA): NK cells were incubated with 20×10^3 trophozoite-stage iRBCs at NK to iRBC ratios of 1:1 and 3:1 in the presence of 20×10^5 uRBCs in 96-well plates for 48 hour at 37°C, in complete medium. Thin blood smears were fixed in 100% methanol, stained with 5% Giemsa solution and counted under light microscope. 25 microscope fields, each containing 200 RBCs, were counted. Parasitemia was expressed as [(number of iRBCs ÷ total number of

RBCs) × 100]. 2.5×10^5 NK cells and 5×10^4 FCR3 VAR2CSA–iRBCs were mixed in 96-well plates and incubated for 6 hour at 37°C in the absence or presence of purified rabbit IgG antibodies to the DBL3 domain (0.5 mg/ml), or purified human IgG antibodies to the DBL domains of PfEMP1 VAR2CSA (0.5 mg/ml), or control rabbit IgG (0.5 mg/ml) in a final volume of 25 µl. A 100-fold excess of uRBCs (5×10^6) was then added, bringing the final volume to 100 µl. Cultures were then maintained for an additional 42 hr at 37°C in standard parasite growth conditions. At the end of incubation, CD45-PE (Clone H130, Biolegend, San Diego, CA) and CD235a-FITC antibodies, and Hoechst were used to stain NK cells, uRBCs and iRBCs. Samples were acquired on FACSLSR-II, and data analyzed with FlowJo (FlowJo, LLC). Parasitemia was determined as the fraction of RBCs ($CD235a^+$) positive for Hoechst. Samples with NK cells but in the absence of antibodies were used as control to calculate growth inhibition.

GIA-ADCC assay: NK cells and iRBCs were resuspended in experimental media (no human serum). 6×10^5 NK cells and 2×10^5 iRBCs were mixed at a 3:1 ratio in 96-well plates and incubated for 6 hour at 37°C in the absence or presence of antibodies. For experiments using plasma, the total amount of plasma in each condition was (20 µl plasma into 200 µl media) to control for the level of plasma. 20 µl of US plasma the negative control, then increasing volume of Mali immune plasma was added in (Example: 2 µl Mali plasma with 18 µl US plasma totaling 20 µl plasma). After a 6 hour coincubation of iRBCs and NK cells, soluble Abs were removed by a wash. This washing step removed any antibody that would bind to merozoites. A 100-fold excess of uRBCs (2×10^7) relative to iRBCs was then added and cultures were maintained for an additional 16 hr at 37°C in standard parasite growth conditions. At the end of incubation, CD45-PE (BD Biosciences), CD235a-FITC, and Hoechst were used to stain NK cells, uRBCs and iRBCs

(supplemental figure S2C). Samples with NK cells but in the absence of antibodies were used as control to calculate growth inhibition.

Hemoglobin release assay: Enriched iRBCs and NK cells were washed with RPMI 1640, containing 0.5 % Albumax in the absence of Phenol red. Cells were mixed at defined ratios in 96-well V bottom plates in 150 µl. Antibodies were added as specified. Antibodies tested in the assay are Rabbit anti-human RBC antibodies (1.25 µg/ml), MGD21 and MGD21-LALA antibodies (Tan et al., 2016) (0.2 mg/ml), Rabbit VAR2CSA and Control IgG antibodies (0.5 mg/ml). Cells were centrifuged at 100g for 3 minutes and incubated at 37°C for 5-6 hours as mentioned. Plate were centrifuged at 2000 rpm for 5 minutes and 50 µl of supernatant was collected. Hemoglobin was measured with QuantiChrom™ Hemoglobin Assay Kit (BioAssay, Hayward, CA). Hemoglobin absorbance was measured at 405 nm using a 96-well plate reader (Enspire, Perkin Elmer, MA and SpectraMax plus, Molecular Devices, CA). In each experiment, maximum hemoglobin release was determined by lysis of iRBCs in 1% Triton-X-100. At the end of the 5 h incubation period, the hemoglobin released in supernatant was quantified as percent fraction of maximum hemoglobin release. Hemoglobin released during the 5 h incubation period in iRBCs sample was subtracted in each experiment to normalize the background in all experiments.

Statistical analysis: Each graph was generated from at least three independent experiments. For normally distributed data, either mean±SD or mean±SEM was used, as specified. Statistical analysis was performed using the software Graphpad Prism v7. Data was analyzed by either two-tailed Student's t test, or by one-way analysis of variance (ANOVA).

Acknowledgments

We thank A. Ring for *P.f.* 3D7 strain enriched for knobs, K. Deitsch for *P.f.* DC-J strain, A. Lanzavecchia for Abs MGD21 and MGD21-LALA, and *P.f.* 3D7 strain enriched for RIFIN expression, B. Hansen for scanning electron microscopy, L. Lantz for IgG purification, J. Skinner for statistics, and A. Sajid for comments on the manuscript.

Additional Information

Competing Interests

L.M.Thomas has employment and equity ownership with Intrexon Corporation. The other authors declare that no competing interests exist.

Funding

Funder

Division of Intramural Research, National Institute of Allergy and Infectious Diseases, National Institutes of Health

Grant reference Z01 AI000525-30 LIG

Author Eric O Long

Author contributions

Conceptualization: G.A., G.T.H., S.K.P., L.H.M., P.D.C., and E.O.L.; Methodology/Design: G.A., G.T.H., J.M.-L., J.B., S.R., L.H.M., S.A.D., and E.O.L.; Investigation: G.A., G.T.H., and J.M.-L.; Resources: J.Y.A.D., D.L.N., L.M.T., O.K.D., B.T., P.E.D., P.D.C., and S.A.D.; Writing –

Original Draft: G.A., G.T.H., and E.O.L.; Writing – Review & Editing: S.R., P.E.D., P.D.C., and S.A.D.; Supervision and Funding Acquisition: S.K.P., L.H.M., P.E.D., P.D.C., S.A.D., and E.O.L.

Author ORCIDS

Eric Long, http://orcid.org/0000-0002-7793-3728

Patrick Duffy https://orcid.org/0000-0002-4483-5005

Ethics

Human subjects: The Ethics Committee of the Faculty of Medicine, Pharmacy, and Dentistry at the University of Sciences, Techniques, and Technologies of Bamako, and the Institutional Review Board of the National Institute of Allergy and Infectious Diseases, National Institutes of Health approved this study. Written informed consent and consent to publish was received from participants prior to inclusion in the study. Written informed consent and consent to publish was obtained from parents or guardians of participating children prior to inclusion in the study. NIAID IRB protocols 07-I-N141 or 06-I-N147.

Additional files

Supplementary files

- Supplementary file 1. Figure S1. Antibody-dependent cytokine response of NK cells in response to iRBCs.
- Supplementary file 2. Figure S2. Assays for NK-dependent parasite growth inhibition.
- Supplementary file 3. Figure S3. Hemoglobin release assay.

519 • Supplementary file 4. Figure S4. PfEMP1 antibodies activate NK-dependent lysis of
520 iRBCs and inhibition of *P.f.* growth.
521 • Supplementary file 5. Table of reagents and Supplementary figure legends.
522 • Supplementary file 6. Movie file M1 shows a co-culture of NK cells, uRBC and iRBC in
523 the presence of US serum, imaged for 104 minutes.
524 • Supplementary file 7. Movie file M2 shows a co-culture of NK cells, uRBC and iRBC in
525 the presence of Mali plasma, imaged for 104 minutes.
526 • Supplementary file 8. Movie file M3 shows a co-culture of NK cells, uRBC and RBC
527 infected with the PfEMP1-deficient *P.f.* strain DC-J in the presence of Mali plasma,
528 imaged for 106 minutes.
529

References

Aley, S. B., Sherwood, J. A., & Howard, R. J. (1984). Knob-positive and knob-negative Plasmodium falciparum differ in expression of a strain-specific malarial antigen on the surface of infected erythrocytes. *J Exp Med, 160*(5), 1585-1590.

Baratin, M., Roetynck, S., Lepolard, C., Falk, C., Sawadogo, S., Uematsu, S., . . . Ugolini, S. (2005). Natural killer cell and macrophage cooperation in MyD88-dependent innate responses to Plasmodium falciparum. *Proc Natl Acad Sci U S A, 102*(41), 14747-14752. doi:10.1073/pnas.0507355102

Bouharoun-Tayoun, H., Oeuvray, C., Lunel, F., & Druilhe, P. (1995). Mechanisms underlying the monocyte-mediated antibody-dependent killing of Plasmodium falciparum asexual blood stages. *J Exp Med, 182*(2), 409-418.

Boyle, M. J., Reiling, L., Feng, G., Langer, C., Osier, F. H., Aspeling-Jones, H., . . . Beeson, J. G. (2015). Human antibodies fix complement to inhibit Plasmodium falciparum invasion of erythrocytes and are associated with protection against malaria. *Immunity, 42*(3), 580-590. doi:10.1016/j.immuni.2015.02.012

Boyle, M. J., Wilson, D. W., Richards, J. S., Riglar, D. T., Tetteh, K. K., Conway, D. J., . . . Beeson, J. G. (2010). Isolation of viable Plasmodium falciparum merozoites to define erythrocyte invasion events and advance vaccine and drug development. *Proc Natl Acad Sci U S A, 107*(32), 14378-14383. doi:10.1073/pnas.1009198107

Bryceson, Y. T., March, M. E., Barber, D. F., Ljunggren, H. G., & Long, E. O. (2005). Cytolytic granule polarization and degranulation controlled by different receptors in resting NK cells. *J Exp Med, 202*(7), 1001-1012.

Bryceson, Y. T., March, M. E., Ljunggren, H. G., & Long, E. O. (2006a). Activation, coactivation, and costimulation of resting human natural killer cells. *Immunol Rev, 214*, 73-91.

Bryceson, Y. T., March, M. E., Ljunggren, H. G., & Long, E. O. (2006b). Synergy among receptors on resting NK cells for the activation of natural cytotoxicity and cytokine secretion. *Blood, 107*(1), 159-166.

Bull, P. C., & Marsh, K. (2002). The role of antibodies to Plasmodium falciparum-infected-erythrocyte surface antigens in naturally acquired immunity to malaria. *Trends Microbiol, 10*(2), 55-58.

560 Cerwenka, A., & Lanier, L. L. (2001). Natural killer cells, viruses and cancer. *Nat Rev Immunol,*
561 *1*(1), 41-49. doi:10.1038/35095564
562 Chan, J. A., Howell, K. B., Reiling, L., Ataide, R., Mackintosh, C. L., Fowkes, F. J., . . . Beeson,
563 J. G. (2012). Targets of antibodies against Plasmodium falciparum-infected erythrocytes in
564 malaria immunity. *J Clin Invest, 122*(9), 3227-3238. doi:10.1172/jci62182
565 Chen, Q., Amaladoss, A., Ye, W., Liu, M., Dummler, S., Kong, F., . . . Chen, J. (2014). Human
566 natural killer cells control Plasmodium falciparum infection by eliminating infected red blood
567 cells. *Proc Natl Acad Sci U S A, 111*(4), 1479-1484. doi:10.1073/pnas.1323318111
568 Cohen, S., Mc, G. I., & Carrington, S. (1961). Gamma-globulin and acquired immunity to human
569 malaria. *Nature, 192*, 733-737.
570 Crompton, P. D., Moebius, J., Portugal, S., Waisberg, M., Hart, G., Garver, L. S., . . . Pierce, S.
571 K. (2014). Malaria immunity in man and mosquito: insights into unsolved mysteries of a deadly
572 infectious disease. *Annu Rev Immunol, 32*, 157-187. doi:10.1146/annurev-immunol-032713-
573 120220
574 Crompton, P. D., Traore, B., Kayentao, K., Doumbo, S., Ongoiba, A., Diakite, S. A., . . .
575 Doumbo, O. K. (2008). Sickle cell trait is associated with a delayed onset of malaria:
576 implications for time-to-event analysis in clinical studies of malaria. *J Infect Dis, 198*(9), 1265-
577 1275. doi:10.1086/592224
578 Doritchamou, J. Y., Herrera, R., Aebig, J. A., Morrison, R., Nguyen, V., Reiter, K., . . . Duffy, P.
579 E. (2016). VAR2CSA Domain-Specific Analysis of Naturally Acquired Functional Antibodies to
580 Plasmodium falciparum Placental Malaria. *J Infect Dis, 214*(4), 577-586.
581 doi:10.1093/infdis/jiw197
582 Douglas, A. D., Williams, A. R., Illingworth, J. J., Kamuyu, G., Biswas, S., Goodman, A. L., . . .
583 Draper, S. J. (2011). The blood-stage malaria antigen PfRH5 is susceptible to vaccine-inducible
584 cross-strain neutralizing antibody. *Nat Commun, 2*, 601. doi:10.1038/ncomms1615
585 Dzikowski, R., Frank, M., & Deitsch, K. (2006). Mutually exclusive expression of virulence
586 genes by malaria parasites is regulated independently of antigen production. *PLoS Pathog, 2*(3),
587 e22. doi:10.1371/journal.ppat.0020022
588 Goncalves, B. P., Huang, C. Y., Morrison, R., Holte, S., Kabyemela, E., Prevots, D. R., . . .
589 Duffy, P. E. (2014). Parasite burden and severity of malaria in Tanzanian children. *N Engl J*
590 *Med, 370*(19), 1799-1808. doi:10.1056/NEJMoa1303944

591 Hill, D. A., Pillai, A. D., Nawaz, F., Hayton, K., Doan, L., Lisk, G., & Desai, S. A. (2007). A
592 blasticidin S-resistant Plasmodium falciparum mutant with a defective plasmodial surface anion
593 channel. *Proc Natl Acad Sci U S A, 104*(3), 1063-1068. doi:10.1073/pnas.0610353104
594 Lambros, C., & Vanderberg, J. P. (1979). Synchronization of Plasmodium falciparum
595 erythrocytic stages in culture. *J Parasitol, 65*(3), 418-420.
596 Malkin, E. M., Diemert, D. J., McArthur, J. H., Perreault, J. R., Miles, A. P., Giersing, B. K., . . .
597 Durbin, A. P. (2005). Phase 1 clinical trial of apical membrane antigen 1: an asexual blood-stage
598 vaccine for Plasmodium falciparum malaria. *Infect Immun, 73*(6), 3677-3685.
599 doi:10.1128/IAI.73.6.3677-3685.2005
600 Mavoungou, E., Luty, A. J., & Kremsner, P. G. (2003). Natural killer (NK) cell-mediated
601 cytolysis of Plasmodium falciparum-infected human red blood cells in vitro. *Eur Cytokine Netw,*
602 *14*(3), 134-142.
603 Mayor, A., Bardaji, A., Macete, E., Nhampossa, T., Fonseca, A. M., Gonzalez, R., . . .
604 Menendez, C. (2015). Changing Trends in P. falciparum Burden, Immunity, and Disease in
605 Pregnancy. *N Engl J Med, 373*(17), 1607-1617. doi:10.1056/NEJMoa1406459
606 Miller, L. H., Baruch, D. I., Marsh, K., & Doumbo, O. K. (2002). The pathogenic basis of
607 malaria. *Nature, 415*(6872), 673-679. doi:10.1038/415673a
608 Obiakor, H., Avril, M., Macdonald, N. J., Srinivasan, P., Reiter, K., Anderson, C., . . . Miller, L.
609 H. (2013). Identification of VAR2CSA domain-specific inhibitory antibodies of the Plasmodium
610 falciparum erythrocyte membrane protein 1 using a novel flow cytometry assay. *Clin Vaccine*
611 *Immunol, 20*(3), 433-442. doi:10.1128/CVI.00638-12
612 Orago, A. S., & Facer, C. A. (1991). Cytotoxicity of human natural killer (NK) cell subsets for
613 Plasmodium falciparum erythrocytic schizonts: stimulation by cytokines and inhibition by
614 neomycin. *Clin Exp Immunol, 86*(1), 22-29.
615 Pieper, K., Tan, J., Piccoli, L., Foglierini, M., Barbieri, S., Chen, Y., . . . Lanzavecchia, A.
616 (2017). Public antibodies to malaria antigens generated by two LAIR1 insertion modalities.
617 *Nature, 548*(7669), 597-601. doi:10.1038/nature23670
618 Rowe, J. A., Moulds, J. M., Newbold, C. I., & Miller, L. H. (1997). P. falciparum rosetting
619 mediated by a parasite-variant erythrocyte membrane protein and complement-receptor 1.
620 *Nature, 388*(6639), 292-295. doi:10.1038/40888

621 Tan, J., Pieper, K., Piccoli, L., Abdi, A., Perez, M. F., Geiger, R., . . . Lanzavecchia, A. (2016). A
622 LAIR1 insertion generates broadly reactive antibodies against malaria variant antigens. *Nature,*
623 *529*(7584), 105-109. doi:10.1038/nature16450
624 Tran, T. M., Li, S., Doumbo, S., Doumtabe, D., Huang, C. Y., Dia, S., . . . Crompton, P. D.
625 (2013). An intensive longitudinal cohort study of Malian children and adults reveals no evidence
626 of acquired immunity to Plasmodium falciparum infection. *Clin Infect Dis, 57*(1), 40-47.
627 doi:10.1093/cid/cit174
628 Wolf, A. S., Sherratt, S., & Riley, E. M. (2017). NK Cells: Uncertain Allies against Malaria.
629 *Front Immunol, 8*, 212. doi:10.3389/fimmu.2017.00212
630 Zhou, J., Feng, G., Beeson, J., Hogarth, P. M., Rogerson, S. J., Yan, Y., & Jaworowski, A.
631 (2015). CD14(hi)CD16+ monocytes phagocytose antibody-opsonised Plasmodium falciparum
632 infected erythrocytes more efficiently than other monocyte subsets, and require CD16 and
633 complement to do so. *BMC Med, 13*, 154. doi:10.1186/s12916-015-0391-7

634

635 **Figure Legends**

636

637 **Figure 1. Primary human NK cells are activated by antibody-coated *P.f.*-iRBCs**. (A)
638 Uninfected RBCs (left) and trophozoite-stage iRBCs (right) were stained with serum pooled from
639 US individuals (red) and plasma pooled from individuals living in a malaria-endemic region of
640 Mali (green). Bound Abs were detected with AF488-conjugated anti-human IgG (H+L) antiserum.
641 (B) Immunofluorescence images of iRBCs stained with DAPI (blue) and with either US serum or
642 Mali plasma, as indicated. Anti-human IgG (H+L) antiserum labeled with AF488 (green) was used
643 to detect Ab-coated RBCs. (C) NK cells stained with PE-Cy5.5-conjugated CD56 and PE-
644 conjugated CD107a Abs. The fraction of $CD107a^+$ NK cells is indicated in each panel. (D) NK
645 cell degranulation measured by CD107a Ab staining. NK cells alone or co-incubated with iRBCs,
646 at a NK:RBC ratio of 1:1 for 4 h, in the absence or presence of Abs, as indicated. Rabbit polyclonal
647 anti-RBC serum (1:4000), US serum (1:10) and Mali plasma (1:10) were used. Circles indicate
648 individual NK cell donors, each with its own color. Data from independent experiments are shown
649 as mean±SD ($p=0.0009$). (E, F) Intracellular staining of IFN-γ and TNF-α. Incubation conditions
650 and Abs as in (D) ($p=0061$ for E, 0.0050 for F). Data from independent experiments are shown as
651 mean±SD.

652

653 **Figure 2. Selective lysis of *P.f.* 3D7-iRBCs and parasite growth inhibition by primary NK**
654 **cells in the presence of immune plasma and IgG.** (A) Live imaging of primary NK cells (green)
655 co-incubated with uRBCs (blue) and iRBCs (red) at an equal ratio (1:1:1) in the presence of US
656 serum (1:10) and of Mali plasma (1:10). Representative snapshots taken at time 0, 2, and 4 h are
657 shown. (B) Quantitative analysis of cell numbers in the cultures shown in (A) in a 3 h period. Cell
658 numbers were normalized to 100 at the start of image acquisition. (C) Composite display of 4

659 independent experiments, each carried out with a different NK cell donor (dotted lines). The mean
660 is shown as a solid line ($p < 0.0001$). (D) Inhibition of parasite growth measured by counting blood
661 smears of iRBCs. A parasite culture containing 1% iRBCs was incubated for 48 h in the absence
662 (open circles) or presence of US serum (closed circles) or Mali plasma (triangles). Growth
663 inhibition is represented as percent decrease in parasitemia relative to a culture with no NK cells
664 and no Ab. Error bars represent standard deviation of the mean from 4 independent experiments
665 ($p<0.0001$ for no NK or US serum group compared with Mali plasma groups in presence of NK
666 cells). (E) Parasite growth inhibition measured by flow cytometry. Enriched trophozoite-stage
667 iRBCs were incubated with NK cells at an NK:iRBC ratio of 3:1 for 6 h with either 20 µl US serum
668 or increasing amounts of Mali plasma in a final volume of 200 µl. Cells were washed and incubated
669 for another 16 h with a 100-fold excess of uRBCs (relative to the iRBC input). Inhibition is
670 expressed as a percent decrease in parasitemia relative to parasitemia in iRBC cultures incubated
671 with NK cells in the absence of Abs ($p=0.0294$). (F) Staining of iRBCs with IgG affinity-purified
672 from US serum at 0.2 (orange) and 0.6 mg/ml (red), or from Mali plasma at 0.2 (blue) and 0.6
673 mg/ml (green). (G) Growth inhibition assay performed as in (E) in the presence of purified IgG
674 from US (black circles) or Mali individuals (green triangles) at the indicated concentrations
675 ($p(0.2)=0.008$; $p(0.6)= 0.003$; $p(1.8) =0.00007$).
676
677 **Figure 3. Naturally acquired antibodies to PfEMP1 have a predominant role in NK-mediated**
678 **ADCC.** (A) Immunostaining of uRBCs with Mali plasma (shaded) and of RBCs infected with *P.f.*
679 3D7 (green) or with *P.f.* DC-J parasites (blue). Bound Abs were detected with AF488-conjugated
680 anti-human IgG (H+L) antiserum. (B) Staining of DC-J iRBCs with Abs from US serum (red) and
681 Mali plasma (green). Secondary staining was as in (A). The shaded histogram represents staining

682 with secondary Ab alone. (C) Live imaging of primary NK cells (green) co-incubated with uRBCs
683 (blue) and DC-J-iRBCs (red) at an equal ratio (1:1:1) in the presence of US serum (1:10) or Mali
684 plasma (1:10). Cell counts for NK cells, DC-J-iRBCs and uRBCs were determined every minute
685 for 3 h. Representative snapshots taken at time 0, 2 and 4 h are shown. (D) Cell numbers were
686 normalized to 100 at the start of image acquisition. Composite display of 4 independent
687 experiments, each carried out with a different NK cell donor (dotted lines). The mean is shown as
688 a solid line. (E) NK cell-mediated ADCC towards uRBCs, *P.f.* 3D7 iRBCs and *P.f.* DC-J iRBCs.
689 Cells were mixed at an NK:RBC ratio of 5:1 and incubated for 5 h in the presence or absence of
690 rabbit anti-RBC serum (1:4000), as indicated. Hemoglobin release, measured using a Quantichrom
691 Hb assay, is shown relative to release from RBCs treated with 1% Triton X-100. Data are shown
692 (mean±SD) for NK cells from 4 independent donors (p=0.6054, comparing 3D7 and DC-J in
693 presence of NK cells and Rabbit anti RBC Ab).
694
695 **Figure 4. Human antibodies to RIFIN and to PfEMP1 promote NK-dependent lysis of iRBCs**
696 **and inhibition of *P.f.* growth.** (A) Staining of RBCs infected with a *P.f.* 3D7 strain enriched for
697 expression of a RIFIN family member (PF3D7_1400600) with human monoclonal Ab
698 MGD21(green) or variant MGD21-LALA (red). The shaded histogram represents staining with
699 AF488-conjugated anti-human IgG (H+L) antiserum alone. (B) Lysis of $RIFIN^{+}$ iRBCs incubated
700 for 6 h in the absence of NK cells or at an NK to iRBC ratio of 5:1 in presence or absence of
701 MGD21 or MGD21 LALA Abs, as indicated. Data are shown (mean±SD) for NK cells from four
702 independent NK cell donors, as measured by Hb release ($p = 0.0005$). (C) Staining of RBCs
703 infected with *P.f.* FCR3 strain expressing VAR2CSA with rabbit polyclonal Ab to the DBL3x
704 domain of PfEMP1 VAR2CSA (green) or with control rabbit serum (red). The shaded histogram

represents staining with secondary FITC-labeled anti-rabbit IgG alone. (D) Hemoglobin release measured after incubation of NK cells with VAR2CSA-iRBCs, at an NK to iRBC ratio of 5:1 for 5 h, in the presence of affinity-purified IgG from control rabbit serum or from serum of rabbit immunized with VAR2CSA PfEMP1. Each color represents a single NK cell donor tested in independent experiments (n=6) ($p = 0.0049$). (E) Staining of iRBCs expressing *P.f.* VAR2CSA with human polyclonal Abs to either AMA1 antigen as control (red), or to the DBL domains of PfEMP1 VAR2CSA (green). The shaded histogram represents staining with AF488-conjugated anti-human IgG (H+L) antiserum alone. (F) Parasite GIA-ADCC analyzed by flow cytometry. Enriched trophozoite-stage FCR3 VAR2CSA-iRBCs were incubated with NK cells, at an NK to iRBC ratio of 5 for 6 h, in the presence of a control rabbit IgG (–), of rabbit anti-PfEMP1 IgG, and of human anti-PfEMP1 IgG, as indicated. A 100-fold excess of uRBCs (relative to the iRBCs input) was added, and incubation resumed for another 42 h. Inhibition is expressed as percent decrease in parasitemia relative to iRBCs that were incubated with NK cells in the absence of Abs ($p = 0.0027$).

Figure 1

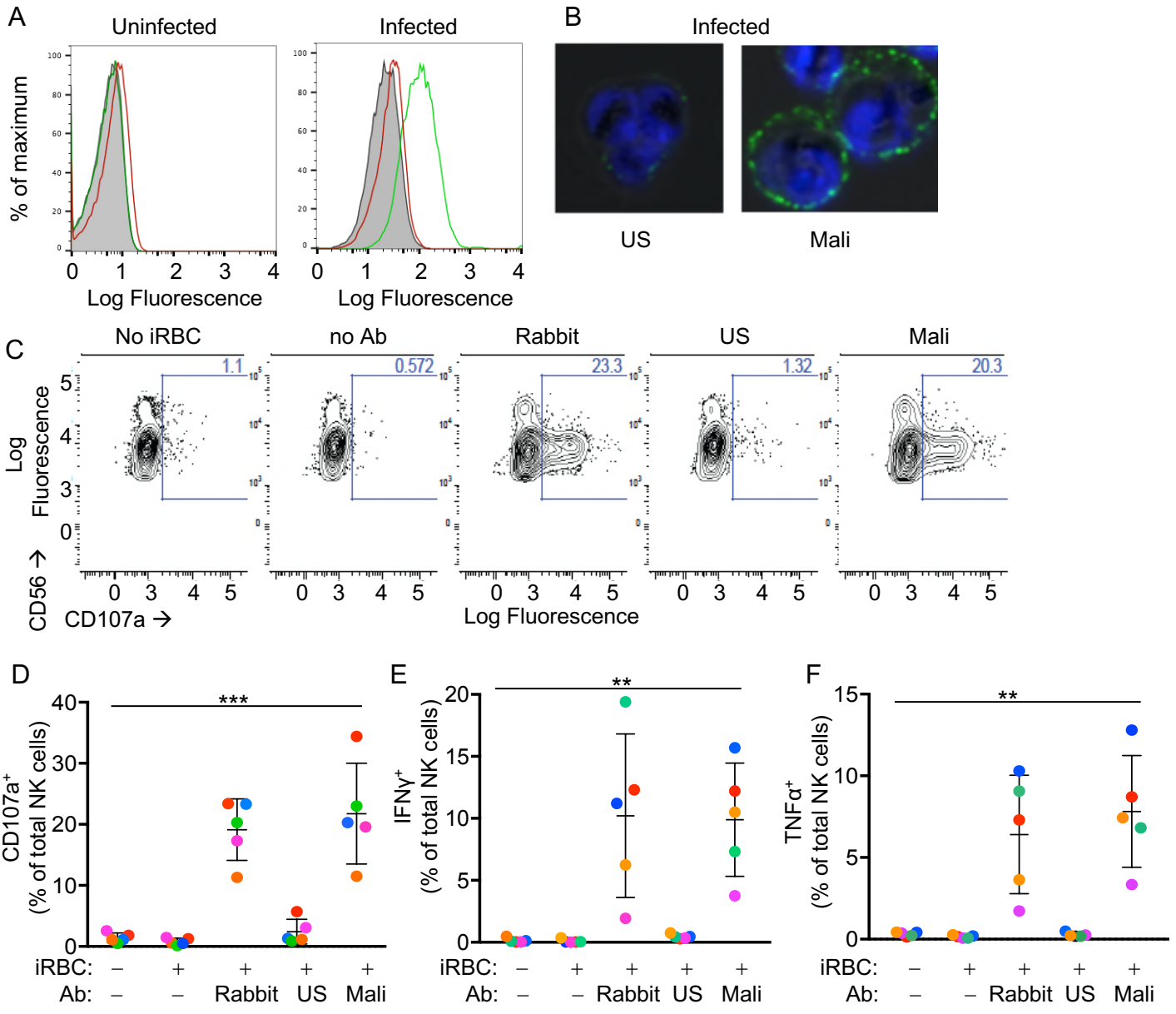
A
Uninfected
Infected
% of maximum
Log Fluorescence
Log Fluorescence
B
Infected
US
Mali
C
No iRBC
no Ab
Rabbit
US
Mali
1.1
0.572
23.3
1.32
20.3
Log Fluorescence
CD56 →
CD107a →
Log Fluorescence
D
E
F
CD107a+ (% of total NK cells)
IFNγ+ (% of total NK cells)
TNFα+ (% of total NK cells)
***
**
**
iRBC: – + + + +
Ab: – – Rabbit US Mali

Figure 2

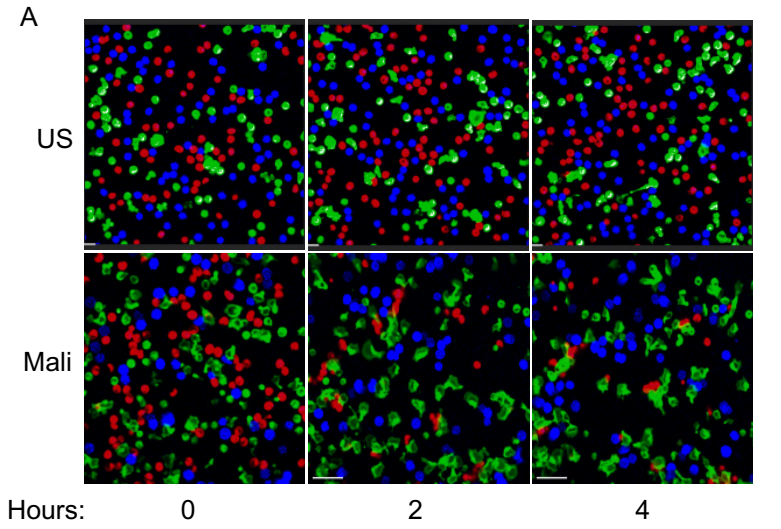
A
US
Mali
Hours: 0 2 4

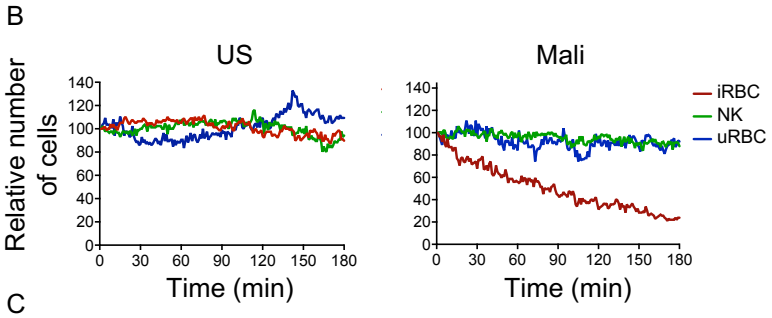
B
US
Mali
Relative number of cells
Time (min)
iRBC
NK
uRBC

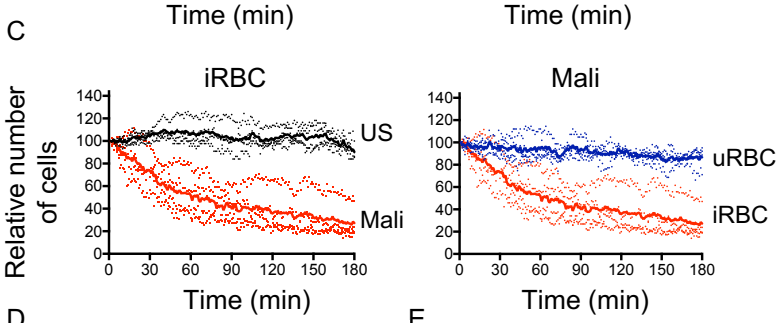
C
iRBC
Mali
Relative number of cells
US
Mali
uRBC
iRBC
Time (min)

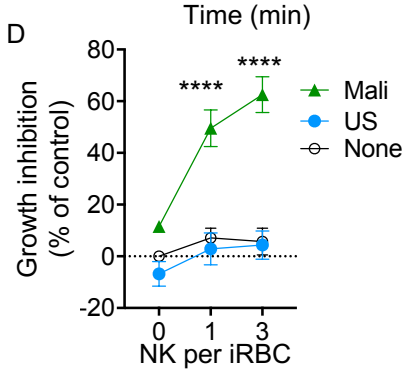
D
Growth inhibition (% of control)
****
****
Mali
US
None
NK per iRBC

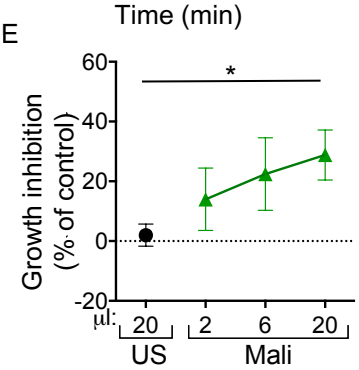
E
Growth inhibition (% of control)
*
µl:
20
2
6
20
US
Mali

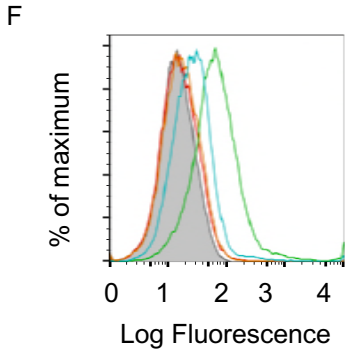
F
% of maximum
Log Fluorescence

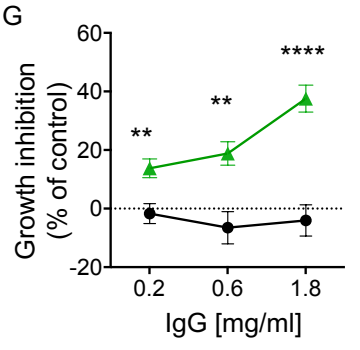
G
Growth inhibition (% of control)
**
**
****
IgG [mg/ml]

Figure 3

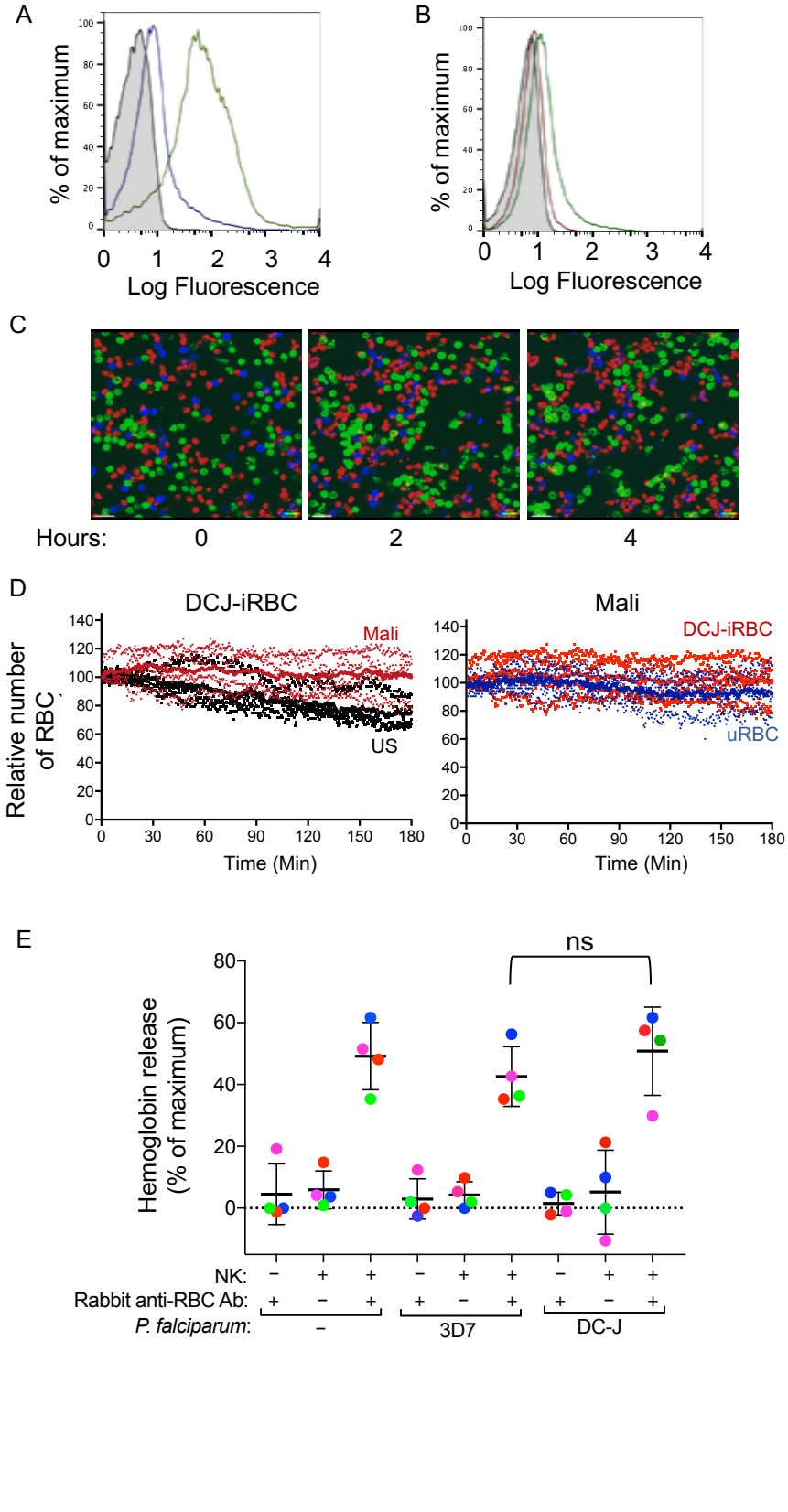
A
% of maximum
Log Fluorescence
B
% of maximum
Log Fluorescence
C
Hours: 0 2 4
D
DCJ-iRBC
Mali
US
Relative number of RBC
Time (Min)
Mali
DCJ-iRBC
uRBC
Time (Min)
E
ns
Hemoglobin release (% of maximum)
NK:
Rabbit anti-RBC Ab:
P. falciparum:
3D7
DC-J

Figure 4

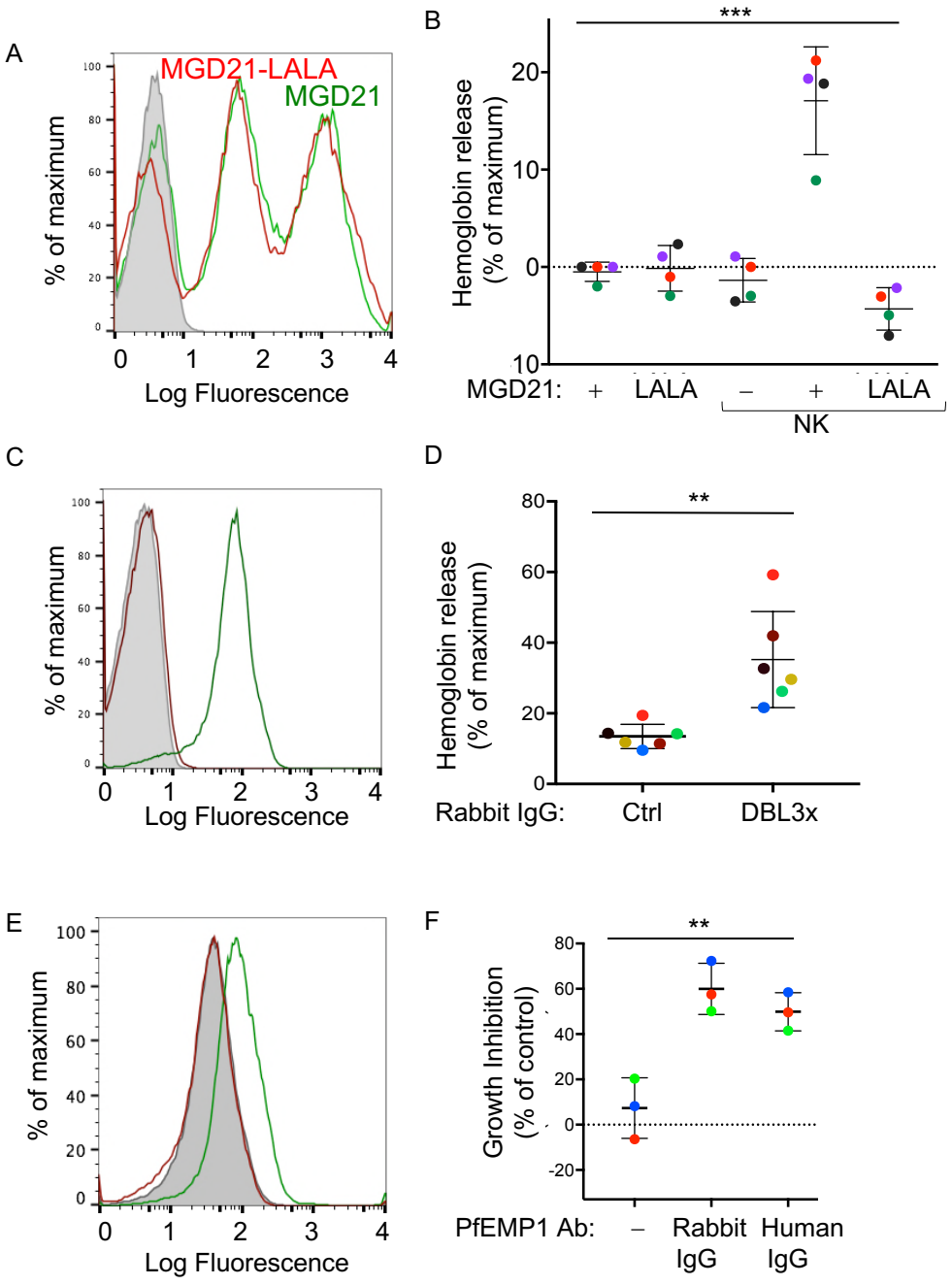
A
MGD21-LALA
MGD21
% of maximum
Log Fluorescence
B
***
Hemoglobin release
(% of maximum)
MGD21: + LALA – + LALA
NK
C
% of maximum
Log Fluorescence
D
**
Hemoglobin release
(% of maximum)
Rabbit IgG: Ctrl DBL3x
E
% of maximum
Log Fluorescence
F
**
Growth Inhibition
(% of control)
PfEMP1 Ab: – Rabbit IgG Human IgG